Method to match waves of ray-tracing simulations with 3-D high-resolution propagation measurements

Method to Match Waves of Ray-Tracing Simulations with 3-D High-Resolution Propagation Measurements

Peng Guo, A. Rainier van Dommele, Matti H.A.J. Herben
Department of Electrical Engineering
Eindhoven University of Technology
Eindhoven, the Netherlands
a.r.v.dommele@tue.nl, m.h.a.j.herben@tue.nl

Abstract—**High-resolution propagation measurements were carried out to verify the angular and delay dispersion predicted by ray-tracing models. To do the comparison between the measured and simulated results, the corresponding waves should first be identified. This paper introduces a method to find the corresponding relationship of waves automatically. The results show that the algorithm can successfully find the matching simulated and measured waves. It also provides the information to find and further investigate the most dominant propagation mechanisms.**

Keywords- angular dispersion; angular spread; delay spread; angle of arrival; deterministic channel modelling

I. INTRODUCTION

For 4G wireless communication systems, the conventional semi-empirical or stochastic propagation prediction models are insufficient for network planning [1]. Time dispersion and angular dispersion in a radio channel are important for the performance of the 4G network. Orthogonal-Frequency Division Multiplexing (OFDM) is applied for modulation in the LTE system. The bandwidth of sub-carriers of the OFDM system is determined by the knowledge of time dispersion in the radio channel. Moreover, smart antennas are used for the 4G networks. These antennas are adaptive arrays or Multiple Input Multiple Output (MIMO) antennas. Angular dispersion due to multipath propagation affects the spatial filter characteristics of the smart antennas. For adaptive antenna arrays, angular dispersion degrades the performance of adaptive beam forming. While for MIMO a wide angular spread of the multipath waves produces a large de-correlation of the spatial channels and hence increases diversity performance. The information of spread in angular domain and time domain cannot be predicted with the conventional empirical propagation models.

Instead deterministic prediction models become more interesting to predict the propagation channels for 4G networks. The ray tracing (RT) model is one of the popular deterministic models nowadays. It uses physical models of radio propagation mechanisms, such as reflection and diffraction, and detailed information of the environment to provide deep insight into the propagation channels [1][2]. This RT model with a detailed building database results in excessive computational complexity, which limits the use by the mobile system operators. Most of the current research in the area of deterministic propagation modelling deals with reducing the computational complexity without losing the prediction accuracy.

The accuracy of deterministic channel modelling is the object of debate and there is still a wide margin for improvements and extensions. The commercially available RT-model has been evaluated through comparison with measurement results. In [3], the results of measurements which were carried out in Rotterdam, the Netherlands are compared with the prediction results based on an RT-model with a maximum of two reflections and one diffraction contribution. The comparison results show that the angular spread and delay spread are not predicted accurate enough by the RT model. The mean error of angular spread prediction is 2 degrees, while the standard deviation of the error is around 16 degrees.

In order to do a more detailed comparison of RT-predictions with measurements, the corresponding propagating electromagnetic waves should be identified firstly. This paper presents a method to find the corresponding waves between measurements and simulations. The comparison is achieved by using the images of measurement and simulation plots in time and space domains, so that a matching method can be designed based on pattern recognition as used in the image processing field.

II. MEASUREMENTS AND SIMULATIONS

The measurement data used for comparison is obtained from outdoor experiments performed with the 3-D high resolution channel sounder developed at TU/e [4]. This system is capable of characterizing the delay and angular properties of mobile radio channels with a resolution better than 5 degrees in both azimuth and elevation domain without ambiguities and while moving through the environment at moderate urban speeds. The time resolution is 20ns with an unambiguous range of 5.1μs. The ray-tracing simulation results in this paper are obtained with the software package CRC-RayPredict [5]. A top-view of the measurement scenario is shown in Fig. 1.

The dynamic measurement and simulation results are plotted in the time and angular domains as a function of snapshot set shown in Fig. 2 and Fig. 3 respectively. The snapshot set number is related to the time elapsed when the vehicle is moving. The vertical noise band in Fig. 2(a)

between snapshot set k=3700 and k=4000 is caused by the saturation of the measurement system.

Fig. 1 Top-view of measurement scenario at TU/e-campus (© Google Maps).

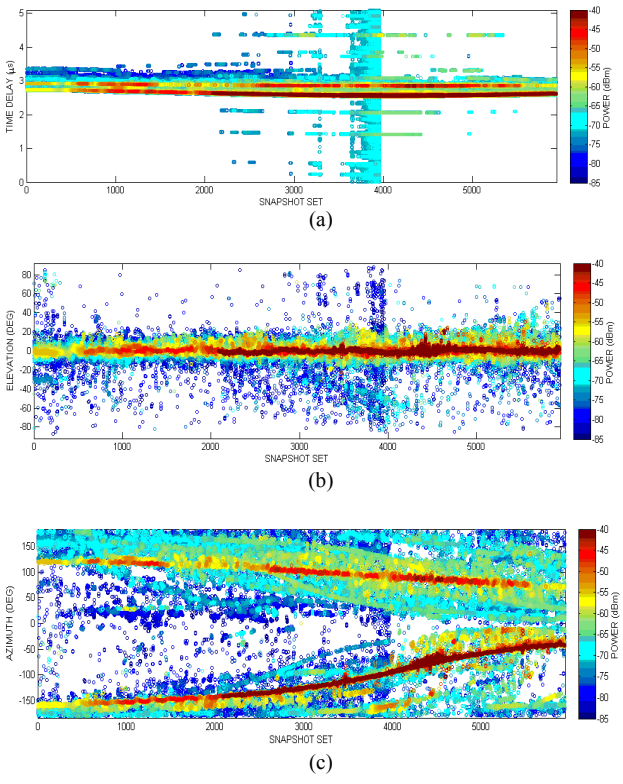

Fig. 2 The measured multipath components at the receiver in (a) time domain, (b) elevation domain (c) azimuth domain along the trajectory.

The most important difference between the simulation and measurement plots is the angular spread due to building surface roughness. In the simulation, only specular reflection happens, resulting in clear lines in the plots along the trajectory. In the measurement, the rough surfaces of the buildings introduce scattering, which contributes to the angular dispersion around the specular reflection waves along the trajectory.

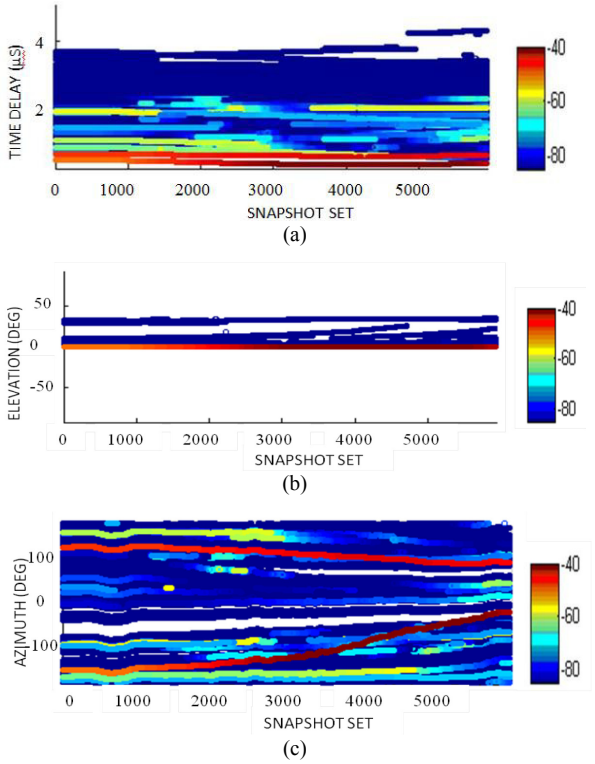

Fig. 3 The simulated multipath components at the receiver in (a) time domain (b) elevation domain (c) azimuth domain along the trajectory.

III. DESCRIPTION OF THE COMPARISON METHOD

The procedure to find the corresponding waves between the simulation and measurement results is based on pattern recognition [6]. This procedure consists of the following steps: clustering, calibration, feature generation, template matching and evaluation, which are shown in Fig. 4.

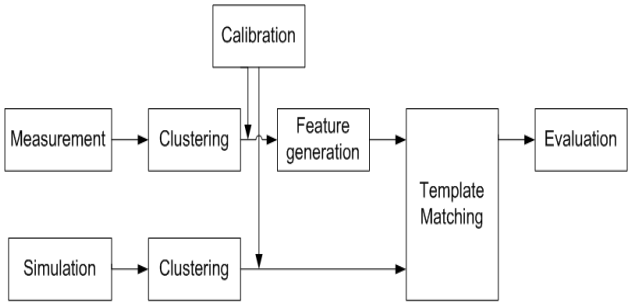

Fig. 4 Procedure to find the corresponding waves in the simulation and measurement results.

A. Clustering

A hierarchical clustering algorithm of the Nearest Neighbourhood is used to cluster the measurement data. The purpose of clustering is to group the measured waves with similar time delay and Angle-of-Arrival (AoA) together [4]. In this way, the specular reflection and the surrounding scattered rays, due to for instance surface roughness, are grouped together. The first 50 measurement clusters with the largest average power are presented in Fig. 5. Different colours indicate different clusters. Due to the limited number of colours, some of them are used repeatedly. Clustering the simulation results can either be done with the same algorithm or by using the information of interaction points of the rays with the reflecting or diffracting objects from the simulator. The simulation results with maximum two reflections are clustered using the same algorithm as that for the measurement, which are shown in Fig. 6.

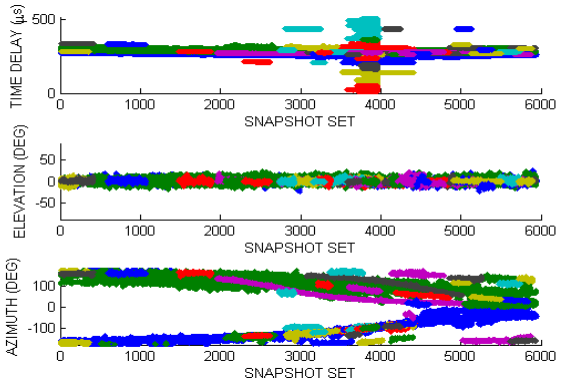

Fig. 5 The first 50 measurement clusters with the largest average power plotted in time, elevation and azimuth domains.

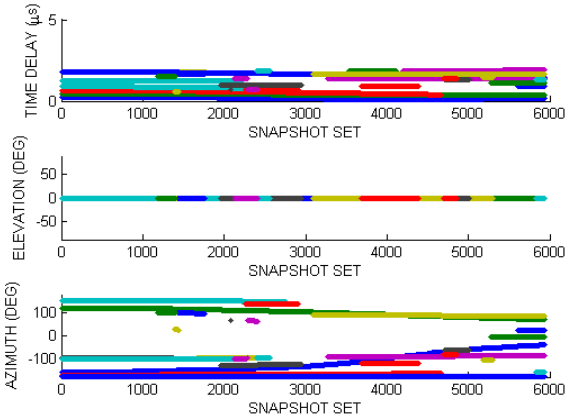

Fig. 6 Clustered simulation results with maximum two reflections plotted in time, elevation and azimuth domains.

B. Calibration

Calibration is necessarily applied to eliminate for instance the time delay offset in the measurements. The start point of time delay in the measurement is chosen arbitrary, because the receiver does not know when the waves depart from the transmitter. The measured time delay is modified based on the theoretical time delay of Line of Sight (LOS) ray that has no reflection loss and can be identified easily. The calibrated measured and simulated delay profiles are shown in Fig. 7.

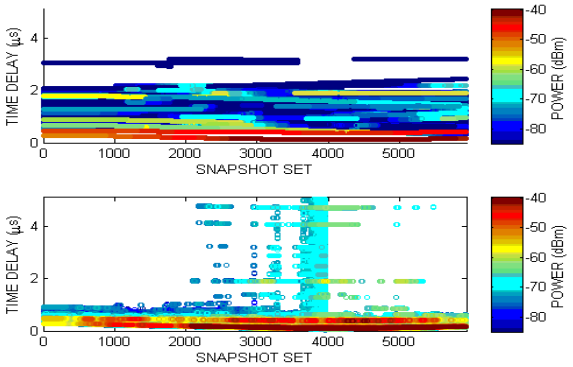

Fig. 7 Simulated delay profile (upper plot) and calibrated measured delay profile (lower plot).

C. Feature Generation

Features of each measured cluster are generated afterwards to eliminate the scattering effect due to surface roughness, so that further comparison is feasible. In this algorithm mean time delay, mean azimuth angle and mean elevation angle are chosen as the features. The values of the features for each measurement cluster at each snapshot set are calculated by Eq.1 [3].

$$\bar{\tau} = \frac{\sum_{i=1}^{n} \tau_i \bullet P_i}{\sum_{i=1}^{n} P_i} \qquad \bar{\phi} = \angle\left(\frac{\sum_{i=1}^{n} e^{j\phi_i} \bullet P_i}{\sum_{i=1}^{n} P_i}\right) \qquad \bar{\theta} = \angle\left(\frac{\sum_{i=1}^{n} e^{j\theta_i} \bullet P_i}{\sum_{i=1}^{n} P_i}\right) \quad (1)$$

where n represents the number of Multipath Components (MPCs) within one cluster at one snapshot set. τ_i, θ_i, ϕ_i and P_i represent the time delay, elevation angle, azimuth angle and received power of the ith MPC out of n MPCs within one cluster at one snapshot set. $\angle$ denotes taking the angle of the complex number.

The plots of the first 50 highest average power clusters with feature values in time and angular domains are shown in Fig. 8. It can be seen that the features of the measurement clusters are represented by lines that later on are compared with the lines of the simulations.

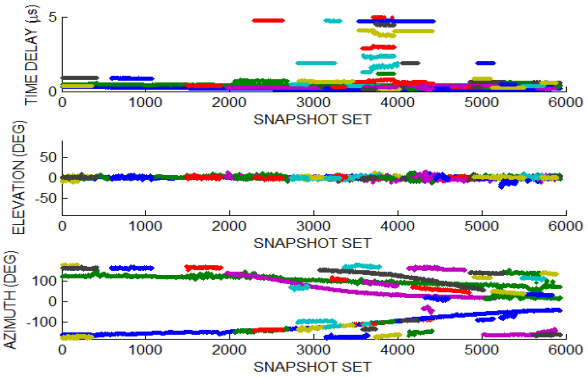

Fig. 8 The mean time delay, mean elevation angle and mean azimuth angle, of the measurement clusters shown in Fig. 5.

D. Template Matching

The procedure of template matching is shown in Fig. 9 to find which one of the simulated clusters (template) matches the measured cluster by using feature values. Assume there are m clusters in the measurement, n clusters in the simulation and k snapshot sets along the trajectory. First choose the objective measurement cluster, e.g. m_i. Then the Euclidean distance is used to measure the difference between the selected measurement cluster and all simulation clusters in time and angular domains. The smaller the Euclidean distance is, the better the selected measurement and chosen simulation cluster match. The Euclidean distance value at each snapshot set is calculated by:

$$(D_j)_k = (\Delta\alpha_j)_k^{\,2} + (\lambda(\Delta\tau_j)_k)^2 \qquad (2)$$

where $(D_j)_k$ is the Euclidean distance, $(\Delta\alpha_j)_k$ is the angular difference and $(\Delta\tau_j)_k$ is the time delay difference between the feature value of measurement cluster m_i and n simulation clusters at each snapshot set k. λ is chosen as the ratio of maximum angle difference value 2π and the maximum time delay difference value 5.1μs to make the influence of them equal on the Euclidean distance. The angle difference $(\Delta\alpha_j)_k$ between objective measurement cluster m_i and individual simulation cluster n_j can be calculated by Eq. 3 [7], using the feature azimuth and elevation angle of objective measurement cluster m_i and the angle values of the individual cluster in the simulation results.

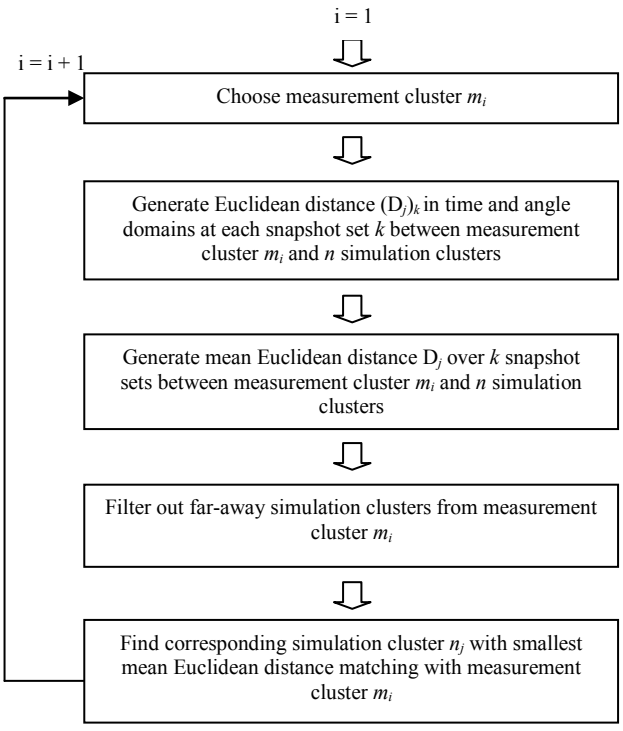

Fig. 9 Procedure of template matching by calculating Euclidean distance.

$$\left(\Delta\alpha_j\right)_k = \cos^{-1}\left\{\begin{pmatrix}\cos\phi_{ik}\cos\theta_{ik}\\ \sin\phi_{ik}\cos\theta_{ik}\\ \sin\theta_{ik}\end{pmatrix}\bullet\begin{pmatrix}\cos\phi_{jk}\cos\theta_{jk}\\ \sin\phi_{jk}\cos\theta_{jk}\\ \sin\theta_{jk}\end{pmatrix}\right\} \qquad (3)$$

After that, the Euclidean distance values are averaged over k snapshot sets to find the difference in a dynamic situation. In the next step, the simulation clusters, which are far from the objective measurement cluster, are filtered out when the angular and time delay difference are larger than a threshold that is based on the measurement resolution. According to the measurement system, the threshold of time delay difference $\Delta\tau$ equals 20ns and angle difference $\Delta\alpha$ equals 5º. In this way, the noise clusters in the measurement (see Fig. 2(a)) can be removed, because there are no simulation clusters nearby. Finally, the simulated cluster n_j with the smallest value of mean Euclidean distance is considered to match the objective measurement cluster m_i. The same procedure is repeated until all the measurement clusters are examined.

IV. Matching Results

Based on the method explained in part III, the matching results for this scenario are listed in Table I.

TABLE I. MATCHING RESULTS INDICATED BY CLUSTER NUMBER

Measurement cluster number	Matching simulation cluster number	Interaction points provided by simulator
1	1	LOS
2	2	Reflection on Traverse building
198,159,103	3	Reflection on IPO building
43,49,99,151, 188,190	4	First reflection on IPO building Second reflection on Traverse building
22,28,57,125	5	First reflection on Traverse building Second reflection on Sports Center building
133	9	First reflection on Traverse building Second reflection on Sports Center building

According to the number of matching measurement clusters, the results can be divided into three categories. First, one measurement cluster can find only one matching simulation cluster, e.g. measurement cluster no. 1 and no. 2. From the interaction points provided by the simulator, it is identified that measurement cluster no. 1 is the LOS wave and cluster no. 2 is the wave with reflection point on the Traverse building. Fig. 10 and Fig. 11 show the plots of measurement and the corresponding simulation clusters, demonstrating the reliability of the matching results. The second category is that several measurement clusters match with the same simulation cluster. For example, there are six measurement clusters that match with simulation cluster no. 4, shown in Fig. 12. This happens when objects exist which are blocking the propagation path for certain parts of the trajectory. Based on the cluster algorithm, the disconnected measurement clusters are regarded as different clusters. Fig. 12 proves the matching results for this situation are also reliable. The last category is that some measurement

clusters have no matching simulation cluster. By checking the plots, it can be found that the noise clusters in the measurement do not match any simulated cluster, as expected. It is also found that some measurement clusters with no matching simulation clusters are formed due to lamppost reflections. For example, by checking the AoA of MPCs superimposed on the video data, the reflection interaction points are the lampposts pointed by the red circles in Fig. 13. This investigation indicates that lamppost reflection plays an important role in a real situation. Therefore, the simulation environment should include the position of lampposts.

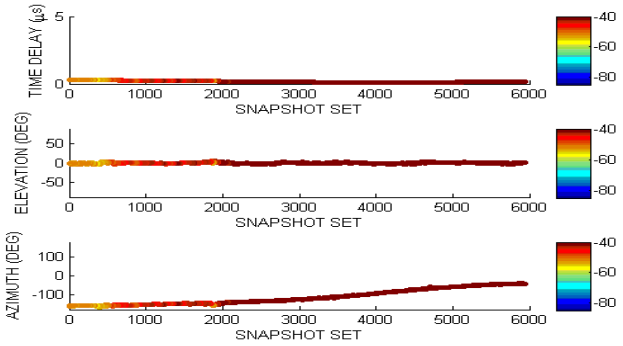

Fig. 10 Feature values of measurement cluster no. 1 and matching simulation cluster no. 1.

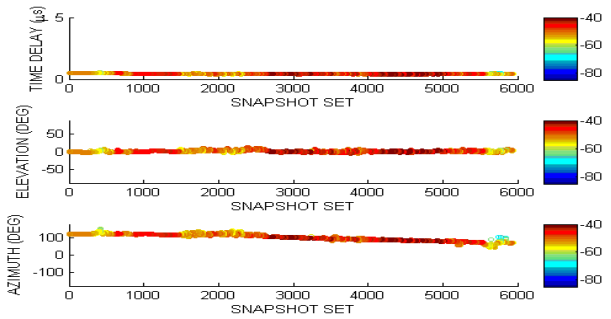

Fig. 11 Feature values of measurement cluster no. 2 and matching simulation cluster no. 2.

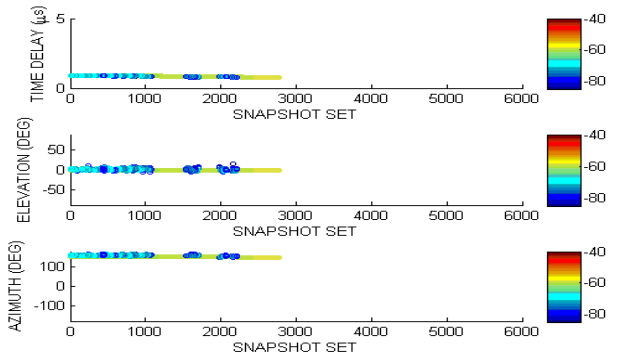

Fig. 12 Feature values of measurement clusters no. 43, 49, 99,151,188,190 and matching simulation cluster no. 4.

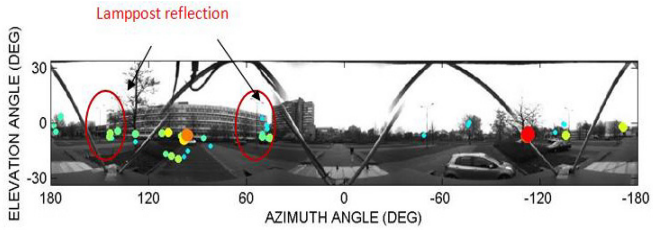

Fig. 13 Angle-of-arrival of multipath components superimposed on omni-directional video data showing lamppost reflections.

Finally, the matching results for the strongest simulated MPCs using the interaction points from Table I are verified with the corresponding video frames at various snapshot sets *k*. This is the evaluation step of the matching procedure (Fig. 4).

V. CONCLUSIONS

In this paper, the corresponding multipath waves between the simulation and measurement results are successfully found by the designed algorithm which consists of five steps: clustering, calibration, feature generation, template matching and evaluation. The Nearest Neighbourhood clustering algorithm can successfully separate the multipath waves related to the physical interacting objects in the measurement. Based on the LOS wave, the time delay offset in measurement results is removed in the calibration step. By generating feature values of measurement clusters, the angular dispersion due to surface roughness in measurements can be eliminated, so that the comparison between the simulation and measurement results can be conducted. The matching plots and the evaluation results prove that the matching results are reliable. It was found that, in addition to LOS and buildings, lampposts play an important role in an urban environment for the angular dispersion of radio waves.

REFERENCES

[1] M.F. Iskander and Z. Yun, "Propagation prediction models for wireless communication system", *IEEE Transanctions on Microwave Theory and Techniques*, Vol. 50, No. 3, Mar. 2002.

[2] L.M. Correia (ed.), "Mobile broadband multimedia networks: techniques, models and tools for 4G", ISBN 0-12-369422-1, May 2006.

[3] O. Mantel, A. Bokiye, A.R. van Dommele and M.R.J.A.E. Kwakkernaat, "Measurement-based verification of delay and angular spread ray-tracing predictions for use in urban mobile network planning", *COST 2100 TD(09) 914*, Vienna, Austria, Sept. 2009.

[4] M.R.J.A.E. Kwakkernaat, "Angular dispersion of radio waves in mobile channels", *PhD thesis,* Eindhoven University of Technology, the Netherlands, 2008, http://alexandria.tue.nl/extra2/200910103.pdf.

[5] The software package CRC-RayPredict was developed by Y.L.C. de Jong at the Communications Research Centre Canada.

[6] S. Theodoris and K. Koutroumbas, "Pattern recognition", Chapter 8, ISBN 0-12-369531-7, 2003.

[7] B. H. Fleury, "First-and second-order characterization of direction dispersion and space selectivity in the radio channel", *IEEE Transactions on information Theory*, Vol. 46, No. 6, Sept. 2000.